

## Adaptive Regulation of Time Varying Disturbances in a Tape Storage System<sup>\*</sup>

Raymond A. de Callafon<sup>\*</sup> Longhao Wang<sup>\*\*</sup>

<sup>\*</sup> *University of California, San Diego, Dept. of Mechanical and Aerospace Engineering, La Jolla, CA 92094-0411 USA (e-mail: callafon@ucsd.edu).*

<sup>\*\*</sup> *University of California, San Diego, Dept. of Mechanical and Aerospace Engineering, La Jolla, CA 92094-0411 USA (e-mail: l3wang@ucsd.edu).*

---

Abstract Archival demands for digital tape storage systems require smaller spacing between data tracks on the magnetic tape to allow for more data storage on a single cartridge. Increasing track density while maintaining track following provides a challenge for the servo control of the tape drive. In particular, interchangeable tape cartridges and time-varying tape reel diameters during operation cause variable disturbances during servo control. In this paper we show how a tape servo control algorithm can be regulated to handle changes in disturbance dynamics during servo operation of the tape drive. The approach is based on adaptive regulation by exploiting a Youla-Kucera parameterization of the servo controller and an explicit minimization of the Position Error Signal (PES) during servo operation in real-time. Theoretical results on the stability of the feedback system and real-time application results on an Linear Tape-Open (LTO) drive are included in the paper. The result show a significant reduction of the variance of the PES over different tape cartridges and a constant PES variance during a complete reel-in operation of the tape drive.

*Keywords:* Servomechanisms, Adaptive control, Recursive estimation, Magnetic data storage

---

### 1. INTRODUCTION

Viable economical and minimal volumetric solutions for data archival storage are being developed in a competitive field of magnetic tape systems. In fact, this year marks the 60th anniversary of IBM's magnetic tape innovation with Linear Tape-Open (LTO) Ultrium 5 tape drives, which can store up to 3 terabytes with a 2:1 compression in a single cartridge. Storing data on magnetic tape remains a competitive economical solution for long-term data storage due to low operational costs, high data reliability, durability and portability of data cartridges and high streaming data rates due multiple-head recording (Reine and Kahn, 2010). The competitive nature of tape storage is due to a combination of pioneering developments in the systems design of tape systems that combine thin-films for tape media, intricate tape transport mechanisms and the use of enhanced servo systems to robustly follow the tracks on the flexible media. Increasing tape cartridge storage capacity can be done by reducing the proximity of adjacent lateral data tracks over the width of a tape and is an essential development for the competitive nature of tape storage as reported by the 2012 INSIC TAPE Roadmap (INSIC, 2012). This proximity of data tracks is identified by the number of data tracks per inch (TPI) and current track densities of approximately 5000 TPI are projected to grow tenfold by 2022.

As flexible tape runs along a magnetic read/write head in a tape drive, a digital Position Error Signal (PES) is available for reducing the relative position of the read/write head with respect to the tape (Pantazi et al., 2012). In current LTO drives, the PES is decoded from dedicated servo tracks on the flexible tape using a timing-based servo pattern and fed back to an digital embedded servo controller to generate control signals for the servo actuator that realigns the read/write head. With Lateral Tape Motion (LTM) during tape transport as one of the main disturbances for data track following, it is clear that a meticulous design of a tape transport mechanism with well-conditioned guides (Kartik, 2006) combined with a high performance control of the servo actuator can support high track densities for a specific tape (Pantazi et al., 2010; Cherubini et al., 2011). However, the portability of cartridges in tape storage poses a daunting challenge: maintain track following and minimize the PES, despite interchangeable cartridges of magnetic flexible tape from different manufactures running at variable speeds.

To minimize the variance of the PES in the presence of unknown and unpredictable LTM, various control solutions have been proposed for tape servo systems. Small form factor servo actuators and optimal control design techniques (Zhou and Doyle, 1997) can be used to increase the bandwidth of the servo system to enable better overall disturbance rejection and reduce PES (Kartik et al., 2011; Lantz et al., 2012). Exploring the possibility of measuring LTM upstream, a combined feedforward/feedback control

---

<sup>\*</sup> Research was sponsored by the INSIC TAPE program.

scheme can be used to improve the track-following performance of the tape head positioning system (Zhong and Pao, 2011). Alternatively, with additional measurements of LTM upstream, tape movement could be mitigated by controllable tape guides (Xia and Messner, 2010). Common and essential in these proposed solutions is a fixed feedback control algorithm that relies on reduction or knowledge of the disturbance dynamics (the size and timing of the LTM) to mitigate the PES during track following. Unfortunately, the LTM is a function of the tape speed and depends on tape cartridge or manufacturer and LTM may even change as a result from external vibrations due to rack mounting or intermittently operating cooling fans in a tape servo system.

Recognizing that the LTM in a tape servo system is a non-stationary disturbances with a time varying spectrum, the contribution of this paper lies in the fact that the performance of an existing tape servo system can be further improved by allowing the feedback control algorithm to *adapt* to the unknown LTM disturbance. Adaptation of feedback to disturbance dynamics is coined Adaptive Regulation by (Landau et al., 2011) and for the special class of periodic disturbances, adaptive regulation can be addressed with Iterative Learning Control (Chen et al., 2007; Tomizuka, 2008). More recently, the ideas of adaptive regulation have been extended to specific classes of periodic disturbances (Landau et al., 2011) and earlier work has demonstrated how such algorithms can be implemented in real-time (Kinney et al., 2011) to allow adaptive regulation of time varying disturbance dynamics, even in the presence of uncertainty in the dynamics of the servo actuator.

The Robust Estimation and Automatic Controller Tuning (REACT) as used in (Kinney et al., 2011) for vibration control and in (Zhong and Pao, 2011) for a tape servo system minimizes the variance of a single performance signal (PES) and leads to minimum variance control solutions (Anderson, 1998) with possible large control signals. In this paper we will show how adaptive feedback regulation can be used to simultaneously minimizes the variance of the PES *and* the control signal of the servo actuator in a tape servo system. Moreover, it is shown that standard Recursive Least Squares (RLS) can be used to perform the simultaneous minimization in the presence of unknown and time-varying LTM disturbances. The adaptive regulation is formulated as a simple "add-on" to an existing feedback controller to facilitate implementation and improve servo performance compared to the existing controller. The "add-on" feature and the RLS allows adaptation of the feedback controller, so the PES can be minimized despite interchangeable cartridges of magnetic flexible tape from different manufactures running at variable speeds. The proposed adaptive regulation is implemented on an actual LTO drive and it is demonstrated how a smaller PES is maintained during track following for complete tape reel-in and reel-out operations for different cartridges.

## 2. ADAPTIVE REGULATION FOR A TAPE SERVO SYSTEM

### 2.1 Servo and Dynamics of an LTO drive

In an Linear Tape Open (LTO) drive, a digital Position Error Signal (PES) is decoded from servo tracks pre-

recorded on the flexible tape using a timing-based servo pattern (Cherubini et al., 2011). Having fast access and maintaining the relative position of the dedicated magnetic servo reading heads with respect to the tape servo patterns is essential to obtain a reliable PES for servo control (Cherubini et al., 2012). As such, the PES is available only when the servo actuator is able to follow the dedicated servo track on the flexible tape in a feedback connection similar to Fig. 1, necessitating the need to perform closed-loop experiments to model servo actuator dynamics on the basis of experimental data.

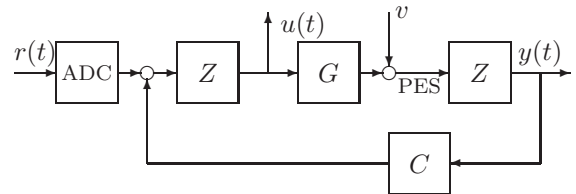


Figure 1. Schematics of closed-loop configuration for the servo control of an LTO drive.

In Fig. 1,  $G$  is used to indicate the servo actuator,  $C$  denotes a existing and known (embedded) servo controller and  $Z$  denotes a Zero Order Hold Digital to Analog Conversion (ZOH DAC). The signal  $v(t)$  indicates the unknown disturbances present on the servo system (such as LTM) that influence the PES during track following. For the discussion of the adaptive regulation of the tape servo system it is important to stress that we assume knowledge of the dynamics of the servo actuator  $G$  and the existing controller  $C$ , whereas not only the LTM disturbances  $v(t)$  is unknown, also its spectrum  $\Phi_v(\omega)$  will be unknown and possibly time varying.

Although the existing controller  $C$  is known due to the user-implemented embedded algorithm, dynamics of the servo actuator  $G$  can be obtained via closed-loop experiments. As indicated in (Wang and de Callafon, 2012), an external reference signal  $r(t)$  via an Analog to Digital Converter (ADC), a measurement of the input signal  $u(t)$  to the actuator and an external measurement of the digital PES  $y(t)$  via ZOH DAC can be used to computing an estimate of the frequency response  $\mathcal{G}(j\omega)$  of the servo actuator  $G$  for curve fitting purposes. Alternatively, simple step experiments on the closed-loop system can be used to formulate a model of the servo actuator using a step-based realization algorithm (Boettcher et al., 2009).

Using the notation  $\Phi_{yr}(j\omega_k)$  to indicate the cross-spectral density function between  $r(t)$  and  $y(t)$  over a frequency grid  $\omega_k$ ,  $k = 1, \dots, N$  the estimate

$$\hat{\Phi}_{yr}(j\omega_k) = \frac{\sum_{l=1}^p Y_l(\omega_k) R_l^*(\omega_k)}{\sum_{l=1}^p R_l(\omega_k) R_l^*(\omega_k)}$$

where the Fourier Transforms  $Y_l(\omega_k) = \sum_{t=1}^N y_l(t) e^{-j\omega_k t}$  and  $R_l(\omega_k) = \sum_{t=1}^N r_l(t) e^{-j\omega_k t}$  are found via the Welch method of averaging an  $N$ -point Fourier transforms (Ljung, 1999) of the signals  $y_l(t)$  and  $r_l(t)$  for different experiments  $l = 1, 2, \dots, p$ . Based on this estimate we can formulate an estimate of the frequency domain data  $\mathcal{G}(j\omega_k)$  of the servo actuator  $G$  via

$$\mathcal{G}(j\omega_k) = Z(j\omega_k)^{-1} \frac{\hat{\Phi}_{yr}(j\omega_k)}{\hat{\Phi}_{ur}(j\omega_k)} \quad (1)$$

where  $Z(j\omega_k)$  denotes the known frequency response of a ZOH DAC.

The frequency response measurements  $\mathcal{G}(j\omega_k)$  can be curve-fitted to formulate a discrete-time model

$$\hat{G}(q, \hat{\theta}) = \frac{b_0 + b_1 q^{-1} + \dots + b_{n_b} q^{-n_b}}{1 + a_1 q^{-1} + \dots + a_{n_a} q^{-n_a}},$$

$$\hat{\theta} = [b_0 \ b_1 \ \dots \ b_{n_b} \ a_1 \ \dots \ a_{n_a}]^T$$

of the servo actuator dynamics by minimizing

$$\hat{\theta} = \arg \min_{\theta} \sum_{k=1}^N |E(\omega_k, \theta)|^2$$

$$E(\omega_k, \theta) = [\mathcal{G}(j\omega_k) - \hat{G}(e^{j\omega_k}, \hat{\theta})]W(\omega_k)$$

using a frequency weighting  $W(\omega_k)$  to emphasize frequency ranges of interests (Raeymaekers et al., 2009).

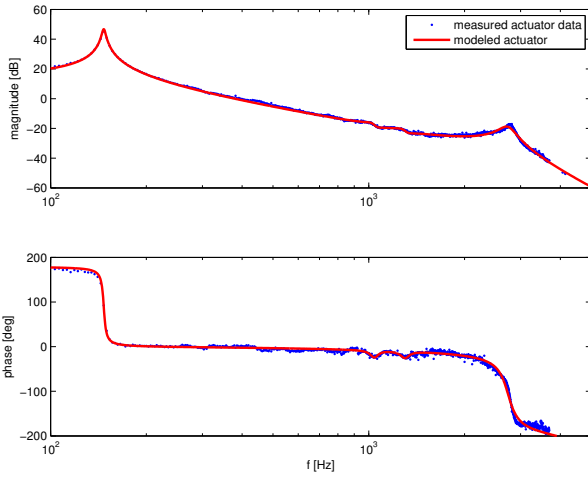


Figure 2. Bode response of the estimated frequency response  $\mathcal{G}(j\omega_k)$  in (1) and the resulting 8rd order model  $\hat{G}(e^{j\omega_k}, \hat{\theta})$ .

The Bode response of the estimated frequency response  $\mathcal{G}(j\omega_k)$  in (1) and the resulting 8th order model  $\hat{G}(e^{j\omega_k}, \hat{\theta})$  found by curve fitting are depicted in Fig. 2. From the plot it can be see that a fairly accurate fit of the measured frequency response is obtained. The model  $\hat{G}$  will be used to represent the knowledge of the dynamics of the servo actuator  $G$  for which we will develop an adaptive regulating controller to minimize the variance of the PES in the presence of an unknown and time-varying LTM disturbances  $v(t)$ .

### 2.2 Initial performance of LTO drive

For the LTO drive we consider in this paper, the existing control algorithm is given by a 6th order discrete-time filter  $C(q)$  operating at 20kHz and given by the transfer function

$$\frac{1.344q^6 + 3.495q^5 - 12.69q^4 + 7.845q^3 + 6.38q^2 - 10.6q + 4.252}{q^6 - 1.251q^5 - 0.3248q^4 + 1.034q^3 - 0.4246q^2 - 0.06697q + 0.03208}$$

The existing controller is a digital PID controller with a high frequency roll-off and an additional notch to suppress the first main resonance mode around 140Hz in the servo actuator.

Implementation of this 6th order discrete-time filter  $C(q)$  operating at 20kHz as indicated above on the LTO drive gives a very reasonable performance of the tape servo

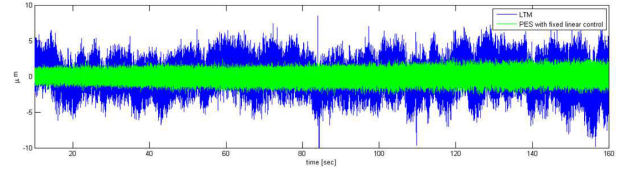


Figure 3. PES and LTM disturbances for an LTO drive with a fixed 6th order linear controller  $C(q)$  at 20kHz using a single tape reel-out while maintaining track following.

system in suppressing LTM disturbances in the PES. The performance of the LTO drive is indicated by the time traces of the PES and the LTM depicted in Fig. 3, where the LTM is reconstructed by a (non-causal) filtering of the PES through the inverse of the sensitivity function  $S = (1 + C\hat{G})^{-1}$ . It should be noted that this reconstructed LTM may not be the actual lateral tape motion in the LTO drive, but only serves as an visual indication of the disturbances present during a tape reel-out as observed by measuring the actual PES from the drive. The initial performance for a fixed linear controller in Fig. 3 provides an important observations: the variance of the PES is not constant during operation. Adaptive regulation will aim to reconstruct the LTM disturbance in real-time and adjust the fixed linear controller to maintain a small PES variance during tape operation.

## 3. ADAPTIVE REGULATION FOR TAPE SERVO

### 3.1 Controller parametrization

A well-know result in controller design and optimization is the Youla parametrization (Anderson, 1998) that allows the parametrization of the class of all stabilizing feedback controllers  $C$  for a given model  $\hat{G}$  by a single stable dynamical perturbation  $Q$ . The Youla parametrization is given in terms of coprime factorization of the model  $\hat{G}$  and the feedback controller  $C$ , but for the scalar and stable transfer functions of the servo dynamics  $\hat{G}$  and the initial feedback controller  $C$  in an LTO drive we can formulate stability as a requirement on the closed-loop transfer functions

$$T(C, \hat{G}) = \begin{bmatrix} C \\ I \end{bmatrix} (I + \hat{G}C)^{-1} [\hat{G} \ I]$$

where  $T(C, \hat{G}) \in \mathcal{RH}_{\infty}$  for internal stability is equivalent to  $\Lambda^{-1} \in \mathcal{RH}_{\infty}$ , with  $\Lambda = 1 + \hat{G}C$  being the inverse of the sensitivity function  $(1 + \hat{G}C)^{-1}$ . For scalar and stable  $\hat{G}$  and  $C$  the Youla parametrization simplifies as follows.

*Definition 1.* Controller Parametrization.

Consider a nominal model  $\hat{G}$  and an initial controller  $C$  with  $T(C, \hat{G}) \in \mathcal{RH}_{\infty}$ . Then all controllers  $C_Q = N_Q D_Q^{-1}$  that satisfy  $T(C_Q, \hat{G}) \in \mathcal{RH}_{\infty}$  are given by

$$C_Q = \frac{C + Q}{1 - \hat{G}Q} \quad (2)$$

The defined controller parametrization indicates that we can vary the perturbation  $Q$  to find new controllers  $C_Q$  for the nominal model  $\hat{G}$ . As long as  $Q \in \mathcal{RH}_{\infty}$  we maintain stability for the feedback of  $C_Q$  and  $\hat{G}$ . The expression

for the new controller  $C_Q$  in (2) also indicates that  $C_Q$  is formed by a simple "add-on" to the existing controller  $C$  as indicated in Fig. 4. We maintain the favorable properties of a previously designed stabilizing feedback controller  $C$  and add on an additional perturbation that uses a model  $\hat{G}$  of the actuator dynamics and a to-be-optimized stable transfer function  $Q$  to further improve the performance of the servo system.

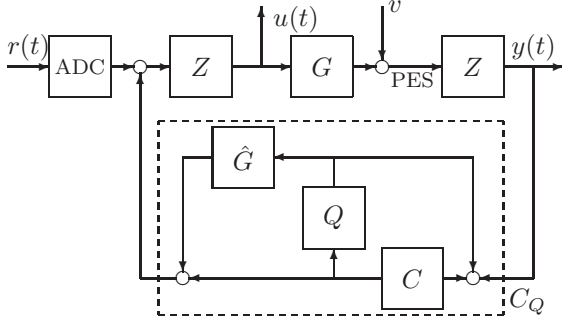


Figure 4. Schematics of closed-loop configuration for the adaptive regulation of an LTO drive.

### 3.2 Mixed performance and control optimization

Next to providing a parametrization of all stabilizing controllers, the controller parametrization in Definition 1 provides another advantage for controller adaptation: all closed-loop transfer functions are linear in the controller perturbation  $Q$ . Considering a feedback system

$$\begin{aligned} y(t) &= \hat{G}u(t) + v(t) \\ u(t) &= -C_Q y(t) \end{aligned} \quad (3)$$

for the adaptive regulation of  $C_Q$  we are concerned with the weighted two-norm performance measure

$$\left\| \begin{array}{c} \gamma u_w \\ y \end{array} \right\|_2 \quad (4)$$

measuring the combined variance of the PES  $y(t)$  and a filtered control signal  $u_w(t) = W(q)u(t)$  as indicated in Fig. 4. The filter  $W(q)$  is a user-specified monic stable filter. Monicity of  $W(q)$  allows us to include an additional scaler weighting  $\gamma$  in the weighted two-norm performance measure of (4).

The variance of  $y(t)$  and  $u(t)$  is driven by the noise disturbance  $v(t) = H(q)e(t)$ , where  $e(t)$  is a white noise signal with a variance  $\lambda$  and  $\Phi_v(\omega) = |H(e^{j\omega})|^2 \lambda$  would be an unknown and possibly time varying spectrum of the noise disturbance. The controller parametrization in Definition 1 allows the weighted two-norm performance measure of (4) to be written in an affine form in the controller perturbation  $Q$ . The result is summarized in the following Corollary.

*Corollary 1.* Consider a nominal model  $\hat{G}$  and an initial controller  $C$  with  $T(C, \hat{G}) \in \mathcal{RH}_\infty$ . Then a controller  $C_Q$  in Definition 1 that minimizes (4) can be computed by

$$\min_{Q \in \mathcal{RH}_\infty} \|W_1 M_{22} W_2 + W_1 M_{21} Q M_{12} W_2\|_2$$

where

$$\begin{aligned} M_{22} &= \begin{bmatrix} C \\ 1 \end{bmatrix} (1 + \hat{G}C)^{-1} [\hat{G} \ 1] = T(C, \hat{G}) \\ M_{21} &= \begin{bmatrix} 1 \\ -\hat{G} \end{bmatrix} \\ M_{12} &= (I + CG)^{-1} [\hat{G} \ I] \\ W_1 &= \begin{bmatrix} -\gamma W & 0 \\ 0 & 1 \end{bmatrix}, \quad W_2 = \begin{bmatrix} 0 \\ H \end{bmatrix} \end{aligned}$$

The proof of Corollary 1 is straightforward by recognizing that with  $1 + \hat{G}C \in \mathcal{RH}_\infty$  we have

$$\begin{aligned} T(C_Q, \hat{G}) &= \begin{bmatrix} C + Q \\ 1 - \hat{G}Q \end{bmatrix} (1 + \hat{G}C)^{-1} [\hat{G} \ 1] \\ &= \begin{bmatrix} C \\ 1 \end{bmatrix} (1 + \hat{G}C)^{-1} [\hat{G} \ 1] + \\ &\quad \begin{bmatrix} 1 \\ -\hat{G} \end{bmatrix} Q (1 + \hat{G}C)^{-1} [\hat{G} \ 1] \end{aligned}$$

and the map from  $e(t)$  to  $[u_w(t) \ y(t)]^T$  is given by  $W_1 T(C_Q, \hat{G}) W_2$ . The affine relation in  $Q$  for the minimization of (4) will be exploited in a (Recursive) Least Squares closed-loop data-based solution in our weighted REACT.

### 3.3 Closed-loop data-based minimization

A data-based solution for minimizing the combined variance of the performance signal  $y(t)$  and a filtered control signal  $u_w(t) = W(q)u(t)$  given in (3) can be formulated based on the closed-loop obtained from the feedback system in (3). The closed-loop data-based solution can be formulated by realizing that we can reconstruct the disturbance  $v(t)$  from the measurements of the PES  $y(t)$ , the control signal  $u(t)$  and using the model  $\hat{G}$ . With  $v(t) = He(t)$ , we can see that

$$(1 + \hat{G}C)^{-1} He(t) = (1 + \hat{G}C)^{-1} y(t) - (1 + \hat{G}C)^{-1} \hat{G}u(t)$$

We now define the filtered closed-loop signal

$$w(t) = (1 + \hat{G}C)^{-1} y(t) - (1 + \hat{G}C)^{-1} \hat{G}u(t) \quad (5)$$

and it should be noted that  $w(t)$  is bounded, as  $(1 + \hat{G}C)^{-1} \in \mathcal{RH}_\infty$  as  $T(C, \hat{G}) \in \mathcal{RH}_\infty$  and  $\hat{G} \in \mathcal{RH}_\infty$ . The signal  $w(t) = (1 + \hat{G}C)^{-1} He(t)$  in (5) basically reconstructs the (filtered) noise signal  $v(t) = He(t)$  via the closed-loop signals  $u(t)$  and  $y(t)$ .

Using the affine relation in the controller perturbation  $Q$  summarized in Corollary 1 allows us to write

$$\begin{aligned} \begin{bmatrix} \gamma u_w(t) \\ y(t) \end{bmatrix} &= \left( \begin{bmatrix} -\gamma WC \\ 1 \end{bmatrix} - \begin{bmatrix} \gamma W \\ \hat{G} \end{bmatrix} Q \right) (1 + \hat{G}C)^{-1} e(t) \\ &= \begin{bmatrix} -\gamma WC \\ 1 \end{bmatrix} w(t) - \begin{bmatrix} \gamma W \\ \hat{G} \end{bmatrix} Q w(t) \end{aligned}$$

Now parameterizing  $Q(\theta)$  we can define an error signal

$$\varepsilon(t, \theta) = \begin{bmatrix} -\gamma WC \\ 1 \end{bmatrix} w(t) - \begin{bmatrix} \gamma W \\ \hat{G} \end{bmatrix} Q(\theta) w(t) \quad (6)$$

that will be linear in the parameter  $\theta$  if and only if  $Q(\theta) \in \mathcal{RH}_\infty$  is parameterized linearly in  $\theta$ . An obvious choice for  $Q(\theta) \in \mathcal{RH}_\infty \forall \theta$  that is parameterized linearly in  $\theta$  would be a Finite Impulse Response (FIR) filter

$$Q(q, \theta) = b_0 + \sum_{k=0}^{\bar{k}-1} b_{k+1} q^{-k-1}, \quad \theta = [b_0 \ b_1 \ \dots \ b_{\bar{k}}] \quad (7)$$

of order  $\bar{k}$ . This parameterization of  $Q(q, \theta)$  allows a convex optimization of (4) over  $\theta$  due to the fact that

$$\begin{aligned} \left\| \begin{matrix} \gamma u_w \\ y \end{matrix} \right\|_2 &= \lim_{N \rightarrow \infty} \frac{1}{N} \sum_{t=1}^N \varepsilon(t, \theta)^T \varepsilon(t, \theta) \\ &= \left\| \begin{bmatrix} -\gamma WC \\ 1 \end{bmatrix} w(t) - \begin{bmatrix} \gamma W \\ \hat{G} \end{bmatrix} Q(\theta) w(t) \right\|_2 \end{aligned} \quad (8)$$

using Parseval's theorem (Ljung, 1999). In conclusion, we can formulate a closed-loop data-based convex optimization of the parameter  $\theta$  in the controller perturbation  $Q(q, \theta)$ , with  $\varepsilon(t, \theta)$  given in (6) and depending solely on the filtered closed-loop signal  $w(t)$  given in (5) and the known initial controller  $C$  and a model  $\hat{G}$  of the servo actuator.

### 3.4 Recursive Solutions

Although the formulation in (8) gives a way to minimize (4) using a standard Least Squares (convex) minimization, the exact minimization of (4) is only achieved in case the number of data points  $N \rightarrow \infty$ . Clearly, such an asymptotic solution is useful if the spectrum  $\Phi_v(\omega) = |H(e^{j\omega})|^2 \lambda$  does not change over time. To anticipate changes in the spectrum  $\Phi_v(\omega)$ , we opt to compute the combined variance of the performance signal  $y(t)$  and a filtered control signal  $u_w(t)$  only over a finite number of time samples and formulate a Recursive Least Squares (RLS) solution.

To formulate an explicit time-dependent recursive solution for the parameter  $\hat{\theta}_t$  of  $Q(q, \hat{\theta}_t)$  via the minimization

$$\begin{aligned} \hat{\theta}_t &= \min_{\theta} \frac{1}{t} \sum_{\tau=0}^t \varepsilon(\tau, \theta)^T \varepsilon(\tau, \theta), \\ \varepsilon(t, \theta) &= y_f(t) - \text{diag}\{Q(\theta)\} u_f(t) \end{aligned} \quad (9)$$

we must first recognize that we can write the error  $\varepsilon(t, \theta)$  into a linear regression form

$$\begin{aligned} \varepsilon(t, \theta) &= y_f(t) - \phi(t)^T \theta \in \mathcal{R}_{2 \times 1}, \quad \text{with} \\ \phi(t)^T &= [u_f(t) \ u_f(t-1) \ \dots \ u_f(t-\bar{k})] \in \mathcal{R}_{2 \times \bar{k}+1} \\ \theta &= [b_0 \ b_1 \ \dots \ b_{\bar{k}}]^T \in \mathcal{R}_{\bar{k}+1 \times 1} \end{aligned}$$

where the regressor  $\phi(t)$  contains past and/or filtered versions of the input signal  $u_f(t)$ . Due to the linear parametrization, the analytic solution to the minimization of (9) can be computed recursively via three iterative steps. The first step is an *a posteriori* prediction error update:

$$\varepsilon(t, \hat{\theta}_{t-1}) = y(t) - \phi(t)^T \hat{\theta}_{t-1} \quad (10)$$

followed by a regularized time weighted covariance update  $P_t$  according to

$$\begin{aligned} P_t &= P_{t-1} + (1 - \lambda_0) I - \\ &P_{t-1} \phi(t) [\phi(t)^T P_{t-1} \phi(t) + I_{2 \times 2}]^{-1} \phi(t)^T P_{t-1} \end{aligned} \quad (11)$$

where  $0 < \lambda_0 \leq 1$  and typically  $\lambda_0$  is chosen close to 1. The regularization has a close relation to Kalman filtering updates when parameters are time varying (Ljung, 1999) and ensure  $P_t > 0$ , even as  $t \rightarrow \infty$ . This means that the parameter estimate  $\hat{\theta}_t$  will not converge to a stationary point, but is able to change at any time  $t$  in case there is a perturbation in the spectrum  $\Phi_v(\omega) = |H(e^{j\omega})|^2 \lambda$  of the noise disturbance  $v(t) = H e(t)$ . Finally, the last step is a parameter update:

$$\hat{\theta}_t = \hat{\theta}_{t-1} + P(t) \phi(t) \varepsilon(t, \hat{\theta}_{t-1}) \quad (12)$$

The recursion can be initialized at  $t = 1$  by  $\theta_0 = 0$  and  $P_0 = \mu I$ ,  $\mu \gg 1$ . Typically, one chooses  $\mu$  to be a large number to allow for fast and aggressive initial parameter updates (Ljung, 1999). However, aggressive parameter updates for  $\mu \gg 1$  do causes large initial fluctuation in  $\theta_t - \theta_{t-1}$ , resulting in possible large control signals  $u(t) = -C_Q y(t)$  during adaptation. To ameliorate the effects of initial parameter conditions during adaptation we employ a simple first order filter

$$\tilde{\theta}_t = (1 - \delta) \hat{\theta}_t + \delta \tilde{\theta}_{t-1} \quad (13)$$

on the parameter updates and implement  $C_Q(q, \tilde{\theta}_t)$  during adaptation instead of  $C_Q(q, \hat{\theta}_t)$ . As the first order filter has a DC-gain of 1, the parameter  $\tilde{\theta}_t$  in (13) will converges to  $\hat{\theta}_t$  in case  $\hat{\theta}_t$  converges to a steady state value.

## 4. APPLICATION OF ADAPTIVE REGULATION TO AN LTO DRIVE

### 4.1 Summary of Algorithm

Following the outline of the algorithm given in the previous section, the adaptive regulation can be summarized as follows. Based on a model  $\hat{G}$  of the servo actuator and knowledge of the initial (embedded) controller  $C$  we formulate an add-on perturbation to the controller  $C$  as indicated in Fig. 4 or (2) to create the perturbed controller  $C_Q$ . We parametrize the filter  $Q(q, \hat{\theta}_t)$  in  $C_Q$  as a Finite Impulse Response (FIR) filter (7) where we choose the order  $\bar{k} = 8$ . The size of  $\bar{k}$  is only limited by the available computational power to implement the recursive estimation of the parameter  $\hat{\theta}_t$  that is solved by the three computational steps for the RLS outlined in (10), (11) and (12). To avoid large fluctuations in FIR filter parameter updates (initial parameter conditions) during adaptation, we update  $Q$  and the controller  $C_Q$  with the filtered parameter  $\tilde{\theta}_t$  in (13).

For the application to the LTO drive we specifically choose  $\hat{\theta}_t = 0$  and  $P_0 = \mu I$ ,  $\mu 10^4$  for initialization,  $\gamma = 0.05$  in (4),  $\delta = 0.995$  in (13) and  $\lambda = 0.995$  in (11). The choice of  $\gamma = 0.05$  was based on experimentation and guaranteed that the control signal  $u(t)$  remained within the bounds of  $\pm 5V$  during adaptation. The choice of  $\delta = 0.995$  ensures limited initial parameter condition effects while still allowing (slow) adaptation due to time-varying disturbances.

### 4.2 Adaptive Regulation Performance of LTO drive

For comparison purposes between fixed linear servo control and servo control with adaptive regulation, we performed the same experiment with the same tape cartridge of a single tape reel-out while maintaining track following as shown earlier in Fig. 3. The comparison with adaptive regulation is depicted in Fig. 5.

From Fig. 5 it can be observed that the PES  $y(t)$  during the adaptive regulation of the controller  $C_Q(q, \tilde{\theta}_t)$  is *smaller* than the PES during a fixed controller experiment. Moreover, the PES variance remains small, even towards the end of the tape reel-out, while the control signal  $u(t)$  slowly and adaptively increases to account for different and/or

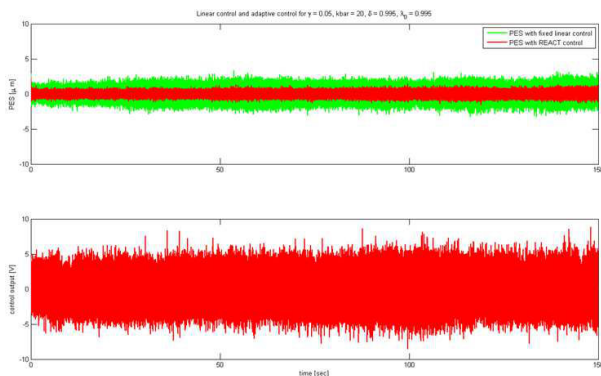


Figure 5. PES disturbances  $y(t)$  (top figure) for a fixed 6th order linear controller  $C(q)$  and an adaptive regulation of the controller  $C_Q(q, \tilde{\theta}_t)$ . Bottom figure shows the control signal  $u(t)$  during the adaptive regulation of the controller  $C_Q(q, \tilde{\theta}_t)$ . Experiment was done at 20kHz using a single tape reel-out while maintaining track following.

larger disturbances towards the end of the tape reel-out. Similar results were observed in our experimental work for different tape cartridges, indicating adaptive features that only can be accomplished with an adaptive regulation feedback control strategy.

## 5. CONCLUSIONS

The paper shows how a tape servo control algorithm can be regulated to handle changes in disturbance dynamics during servo operation of the tape drive. The approach is based on adaptive regulation by exploiting a Youla parameterization of the servo controller and an explicit minimization of the Position Error Signal (PES) during servo operation in real-time. Theoretical results on the parametrization of the feedback controller and stability of the feedback system indicate that the adaptive controller can be implemented as a simple "add-on" to an existing embedded fixed feedback control algorithm. The real-time application results on an Linear Tape-Open (LTO) drive show a significant reduction of the variance of the PES over different tape cartridges and a constant PES variance during a complete reel-in/out operation of the tape drive.

## REFERENCES

- Anderson, B. (1998). From Youla-Kucera to identification, adaptive and nonlinear control. *Automatica*, 34, 1485–1506.
- Boettcher, U., Raeymakers, B., de Callafon, R., and Talke, F. (2009). Dynamic modeling and control of a piezoelectric dual-stage tape servo actuator. *IEEE Transactions on Magnetics*, 45, 3017–3024.
- Chen, Y.Q., Moore, K., Yu, J., and Zhang, T. (2007). Iterative learning control and repetitive control in hard disk drive industry - a tutorial. *Int. J. Adapt. Control and Signal Processing*, 22, 325–343.
- Cherubini, G., Cideciyan, R., Dellmann, L., Eleftheriou, E., Haeberle, W., Jelitto, J., Kartik, V., Lantz, M., Ölçer, S., Pantazi, A., Rothuizen, H., Berman, D., Imano, W., Jubert, P., McClelland, G., Koeppe, P., Tsuruta, K., Harasawa, T., Murata, Y., Musha, A., Noguchi, H., Ohtsu, H., Shimizu, O., and Suzuki, R. (2011). 29.5-Gb/in<sup>2</sup> recording areal density on Barium Ferrite tape. *IEEE Tran. on Mag.*, 47, 137–147.
- Cherubini, G., Jelitto, J., and Tsuruta, K. (2012). Fast servo signal acquisition in tape drives using servo and data channels. *Mechatronics, Elsevier*, 22, 349–360.
- INSIC (2012). Insic 2012-2022 international magnetic tape storage roadmap. Technical report, INSIC.
- Kartik, V. (2006). *In-plane and Transverse Vibration of Axially-moving Media with Advanced Guiding and Actuation Elements*. Ph.D. thesis, Carnegie Mellon University.
- Kartik, V., Pantazi, A., and Lantz, M. (2011). Track-following high frequency lateral motion of flexible magnetic media with sub-100 nm positioning error. *IEEE Tran. of Mag.*, 47, 1868–1873.
- Kinney, C., Fang, H., de Callafon, R., and Alma, M. (2011). Robust estimation and automatic controller tuning in vibration control of time varying harmonic disturbances. In I. Milan (ed.), *Prepr. 18th IFAC World Congress*, 5401–5406.
- Landau, I., Lozano, R., M'Saad, M., and Karimi, A. (2011). Adaptive regulation - rejection of unknown disturbances. *Communication and Control Engineering*, 477–497.
- Lantz, M., Cherubini, G., Pantazi, A., and Jelitto, J. (2012). Servo-pattern design and track-following control for nanometer head positioning on flexible tape media. *IEEE Transactions on Control Systems Technology*, 20, 369–381.
- Ljung, L. (1999). *System Identification-Theory for the User*. Prentice-Hall, Englewood Cliffs, NJ USA, second edition.
- Pantazi, A., Jelitto, J., and Bui, N. Ans Eleftheriou, E. (2010). Track-follow control for tape storage. In *Proc. 5th IFAC Symp. Mechatronics Systems*, 532–537. Cambridge, MA.
- Pantazi, A., Jelitto, J., Bui, N., and Eleftheriou, E. (2012). Track-following in tape storage: Lateral tape motion and control. *Mechatronics, Elsevier*, 22, 361–367.
- Raeymakers, B., Graham, M., de Callafon, R., and Talke, F. (2009). Design of a dual stage actuator tape head with high-bandwidth track following capability. *Microsystem Technologies*, 15, 1525–1529.
- Reine, D. and Kahn, M. (2010). In search of the long-term archiving solution - tape delivers significant tco advantage over disk. In *Clipper Notes*.
- Tomizuka, M. (2008). Dealing with periodic disturbances in controls of mechanical systems. *Annual Reviews in Control*, 32, 193–199.
- Wang, L. and de Callafon, R. (2012). Modeling and estimation of servo actuator dynamic variability with application to lto-drives. In *Proc. IEEE/ASME International Conference on Advanced Intelligent Mechatronics (AIM)*, 796–801.
- Xia, L. and Messner, W. (2010). Active tape steering control system. *IFAC Journal Mechatronics*, 20, 6–11.
- Zhong, H. and Pao, L. (2011). Combined feedforward/feedback control for tape head track-following servo systems. In *Preprints of the 18th IFAC World Congress*, 4040–4045. Milan, Italy.
- Zhou, K. and Doyle, J. (1997). *Essentials of Robust Control*. Prentice Hall, Upper Saddle River, NJ.